Cyclometalated Complexes of Platinum and Palladium with *N*-(4-Chlorophenyl)-α-benzoylbenzylideneamine. *In Vitro* Cytostatic Activity, DNA Modification, and Interstrand Cross-Link Studies

Carmen Navarro-Ranninger,*,† Isabel López-Solera,† Víctor M. González,‡ José M. Pérez,‡ Amparo Alvarez-Valdés,† Avelino Martín,§ Paul R. Raithby,§ José R. Masaguer,† and Carlos Alonso*,‡

Departamento de Química Inorgánica and Centro de Biología Molecular "Severo Ochoa", Facultad de Ciencias, Universidad Autónoma de Madrid, 28049-Madrid, Spain, and Department of Chemistry, University of Cambridge, Lensfield Road, Cambridge CB2 1EW, U.K.

Received January 17, 1996[⊗]

In the present paper we report the synthesis and structural IR and ^{1}H and ^{13}C NMR characterization of four platinum(II) and palladium(II) cyclometalated complexes of the formula $[Pd(4\text{-}ClC_6H_4N{=}C(COC_6H_5)C_6H_4)X]_2$, where X = OAc (**2**) or Cl (**3**), and $[Pt(4\text{-}ClC_6H_4N{=}C(COC_6H_5)C_6H_4)X]_2$, where X = Cl (**4**) or OAc (**5**). The acetate-bridged compounds **2** and **5** have an open-book structure. The chloro-bridged compounds **3** and **4** have an unfolded structure. Complex **2** crystallizes in the centrosymmetric triclinic space group $P\bar{1}$, with $Z = 2$. Unit cell parameters are as follows: $a = 11.765(3)$ Å, $b = 12.862(4)$ Å, $c = 15.022(5)$ Å, $\alpha = 84.08(2)°$, $\beta = 78.56(2)°$, $\gamma = 83.13(2)°$. All these compounds were screened against MDA-MB 468 (breast carcinoma) and HL-60 (leukemic) tumor cells. The low IC_{50} values of compound **5** (1.05 μM) and of compound **4** (1.58 μM) against MDA-MB 468 and of 0.82 μM (**5**) and 1.37 μM (**4**) against HL-60 relative to *cis*-DDP (2.67 and 2.07 μM, respectively) and other cyclometalated compounds suggest that the synthesized compounds may be regarded as having potential antitumor properties. The data suggest that the antiproliferative activity of compound **5** may correlate with its covalent binding to DNA and the induction of important modifications on the helix.

I. Introduction

Since the detection of the antitumor activity of *cis*-dichlorodiammineplatinum (*cis*-DDP), a wide range of analogous compounds with the general formula ML_2X_2 have been synthesized and characterized.[1−5] By alteration of the nature of the metal M, the kinetically inert ligands L, or the kinetically labile ligands X, the kinetic, structural, and electronic properties of the molecules can be "fine-tuned" to maximize the activity of these complexes. Thus, the search for systems with antitumor activity has been extended to a whole range of coordination and organometallic compounds and even to compounds which do not contain metals.[6] Our interest in this area has been focused on complexes analogous to *cis*-DDP, where the ligands X and L have specific properties (where L is a derivative of benzoylbenzylideneamine which allows cyclometalation reactions and where X is either chlorine or acetate).[7,8] The present study is based on the following facts: (1) Pd and Pt cyclometalated complexes with benzoylbenzylideneamines display high antitumor activity, showing specific activity towards some forms of cancer.[9] (2) Different optical isomers of these compounds show different levels of antitumor activity.[10] (3) The palladium and platinum cyclometalated complexes containing carboxylate with a folded structure show greater activity than complexes containing chloride with an unfolded structure.[9] (4) Different substituents on the ligand modify the reactivity of the resulting complexes. (5) The palladium and platinum complexes produce conformational changes in the double helix of DNA.[11] In order to perform a further analysis of the influence of some of these factors on the biochemical properties of cyclometalated complexes, we have synthesized new compounds which contain activated ligands having a chloro substituent, *N*-(4-chlorophenyl)-α-benzoylbenzylideneamine. The activity of the newly synthesized compounds has been compared with the activity of related Pd(II) and Pt(II) cyclometalated complexes previously described,[9] showing that the former exhibit higher antiproliferative activity. Our studies suggest that the biochemical mode of action of compound **5** may be due to the formation of monofunctional or bifunctional intrastrand adducts on DNA and that it does not induce interstrand cross-linking.

II. Results and Discussion

Synthesis and Characterization. The reaction of equimolar amounts of $Pd(OAc)_2$ with the ligand *N*-(4-chlorophenyl)-α-benzoylbenzylideneamine (**1**) in HOAc resulted in the formation of the acetate-bridged cyclometalated compound **2**. The

* To whom correspondence should be addressed.
† Departamento de Química Inorganica, Universidad Autónoma de Madrid.
‡ Centro de Biología Molecular "Severo Ochoa", Universidad Autonóma de Madrid.
§ University of Cambridge.
⊗ Abstract published in *Advance ACS Abstracts,* August 1, 1996.

(1) Reedijk, J. *Inorg. Chim. Acta* **1992**, *198*, 873.
(2) Köft-Maier, P. *Chem. Rev.* **1987**, *87*, 1137.
(3) Hollis, S. L.; Amundsen, A. R.; Stern, E. W. *J. Med. Chem.* **1989**, *32*, 128.
(4) Farrell, N.; Hacker, M. P. *J. Med. Chem.* **1990**, *33*, 2179.
(5) Pasini, A.; Zunino, F. *Angew. Chem.* **1987**, *26*, 615.
(6) Keppler, B. K. *New J. Chem.* **1990**, *14*, 389.
(7) García-Ruano, J. L.; López-Solera, I.; Masaguer, J. R.; Navarro-Ranninger, C.; Rodríguez, J. H. *Organometallics* **1992**, *11*, 3013.
(8) Navarro-Ranninger, C.; López-Solera, I.; Alvarez-Valdés, A.; Rodríguez-Ramos, J. H.; Masaguer, J. R.; García-Ruano, J. L. *Organometallics* **1993**, *12*, 4104.
(9) Navarro-Ranninger, C.; López-Solera, I.; Pérez, J. M.; Rodríguez, J.; García-Ruano, J. L.; Raithby, P. R.; Masaguer, J. R.; Alonso, C. *J. Med. Chem.* **1993**, *36*, 3795.
(10) Navarro-Ranninger, C.; López-Solera, I.; Pérez, J. M.; Masaguer, J. R.; Alonso, C. *Appl. Organomet. Chem.* **1993**, *7*, 57.
(11) Navarro-Ranninger, C.; Amo-Ochoa, P.; Pérez, J. M.; González, V. M.; Masaguer, J. R.; Alonso, C. *J. Inorg. Biochem.* **1994**, *53*, 177.

S0020-1669(96)00050-X CCC: $12.00

Scheme 1

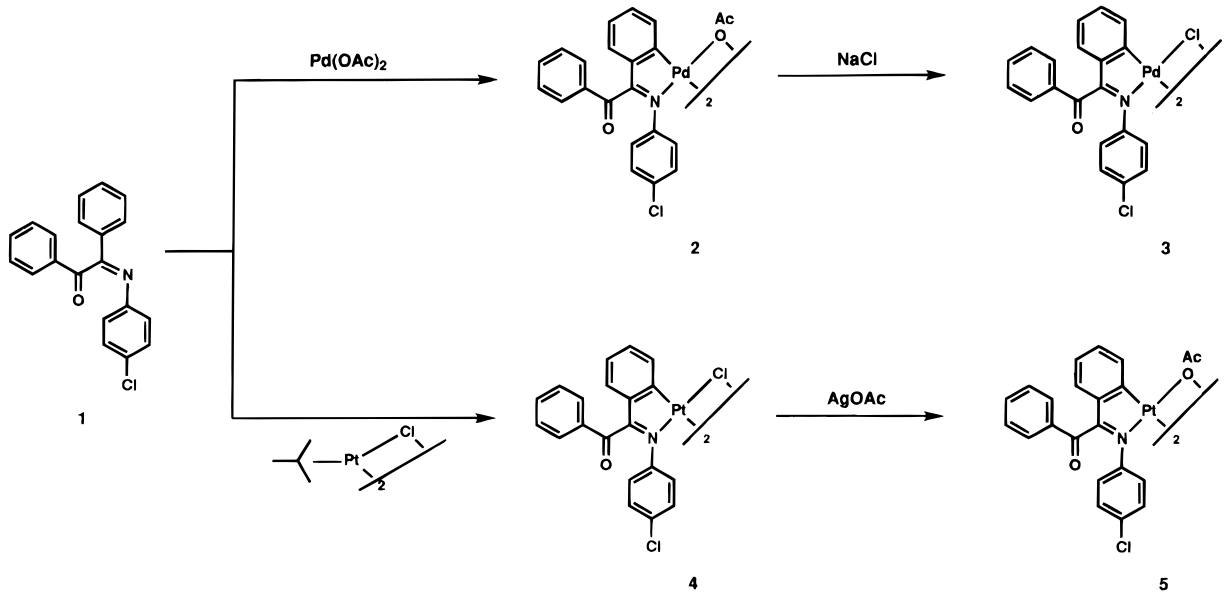

posterior metathetical reaction of this compound with NaCl led to the formation of the chloro-bridged compound **3**, which can also be obtained by reaction of the ligand with $PdCl_2$ in MeOH. The ortho-platinated compound **4** was obtained from $[Pt(\mu\text{-}Cl)_2(\eta^3\text{-}C_4H_7)_2]$ using $CHCl_3$ as solvent.[12] The chloro-bridged complex **4** was converted into the acetate-bridged form (compound **5**) by treatment with silver acetate in $CHCl_3$ (Scheme 1). All the compounds are air stable. The acetate dimers, compounds **2** and **5**, are soluble in most organic solvents. The chloro derivatives, compounds **3** and **4**, are slightly soluble in organic solvents such as $CHCl_3$ but soluble in DMSO and DMF. The microanalytical data of compounds **2**, **3**, **4**, and **5** (see Experimental Section) are consistent with the empirical formula $[M(4\text{-}ClC_6H_4N{=}C(COC_6H_5)C_6H_4)X]$ (M = Pd, X = OAc, **2**; M = Pd, X = Cl, **3**; M = Pt, X = Cl, **4**; M = Pt, X = OAc, **5**).

The IR analysis showed that the bands assigned to the ν(C═O) stretching frequencies remain unchanged in all the compounds relative to the ligand. The presence of negative shifts in the ν(C═N) stretching frequency and of a band assignable to ν(M−N) about 450 cm^{-1} in all compounds suggests that the ligand coordinates to the metal through the nitrogen. The IR spectra of complexes **2** and **5** exhibit the typical asymmetric and symmetric stretching modes of the acetate groups with strong absorptions at 1584 and 1421 cm^{-1} for compound **2** and at 1584 and 1418 cm^{-1} for compound **5**. The IR spectrum of compound **3** exhibits, on the other hand, two asymmetric ν(Pd−Cl) stretching absorptions at 319 and 295 cm^{-1}. Also, compound **4** exhibits two ν(Pt−Cl) stretching absorptions at 328 and 324 cm^{-1}.

The ^1H NMR data for ligand **1** and their ortho-palladated derivatives compounds **3** and **4** are shown in Table 1. For compounds **2** and **5**, see the Experimental Section. The spectra were assigned on the basis of chemical shifts and of spin−spin coupling information and were confirmed by selective proton decoupling. The *trans* arrangement of the ligands in the acetates **2** and **5** is inferred from the fact that the acetate-bridge methyl groups appear as singlets at 1.80 and 1.95 ppm, respectively. The presence of a broadened unresolved pattern in the aromatic region can explain the open-book-shape structure of the

(12) Pregosin, P. S.; Wombacher, F.; Albinati, A.; Linaza, F. *J. Organomet. Chem.* **1991**, *418*, 249.

Table 1. ^1H NMR Spectral Parameters (δ, ppm)[a] for Ligand **1** and Compounds **3** and **4** in DMSO-d_6

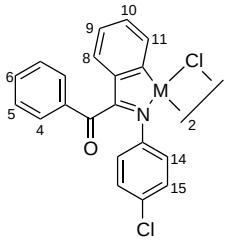

	1	**3** (M = Pd)	**4** (M = Pt)
H4,4′	7.87, m, 2H	7.81, m, 2H	7.81, m, 2H
H5,5′	7.38, m, 2H	7.51, m, 2H	7.52, m, 2H
H6	7.42, m, 1H	7.70, m, 1H	7.71, m, 1H
H8	7.75, m, 2H	6.90, d (7.3), 1H	7.01, dd (1.2,7.6), 1H
H9	7.28, m, 2H	7.03, t (7.3), 1H	7.35, dt (1.2, 7.6), 1H
H10	7.43, m, 1H	7.18, m, 1H	7.13, dt (1.2, 7.6), 1H
H11		7.84, m, 1H	8.31,[b] dd (1.2, 7.6), 1H
H14,14′	6.38,[c] 2H	7.14,[c] 2H	7.30−7.00, m
H15,15′	7.06,[c] 2H	7.28,[c] 2H	7.30−7.00, m

[a] Abbreviations: d, doublet; t, triplet; dd, double doublet; dt, double triplet; m, multiplet. The numbers in parentheses correspond to $J(^1H-^1H)$ in Hz. [b] $^3J(^{195}Pt-^1H) = 39.1$ Hz. [c] AA′BB′ system.

compounds, as suggested by the X-ray data of similar complexes[7] and by the X-ray diffraction data of compound **2** (see below). In contrast, the ^1H NMR spectra of complexes **3** and **4** show well-resolved patterns in the aromatic region, indicating the unfolded structure of these complexes. The main difference between the spectra of the isostructural compounds **3** and **4** is the larger chemical shift observed for H11 (7.84 ppm in **3** and 8.31 ppm in **4**). This suggests that the platinum atom has a stronger deshielding effect than palladium on the *ortho* position. The strong shielding effect at H8 must be a consequence of the change in the spatial arrangement of the COC_6H_5 group of the cyclometalated complexes, with respect to that exhibited by the ligand. The signal corresponding to H11 in Pt compound **4** shows a splitting due to the coupling with the metal ($^3J(^{195}Pt-^1H) = 39.1$ Hz).

The ^{13}C NMR parameters of ligand **1** and those of the palladium and platinum compounds are shown in Table 2. The spectra were assigned by heteronuclear 2D correlation spectroscopy,[13] and the quaternary carbon atoms were assigned by the heteronuclear NOE effect.[14] The spectra of the palladium

Table 2. ^{13}C NMR Parameters (δ, ppm)[a] of the Ligand **1** and Complexes **2**−**5**

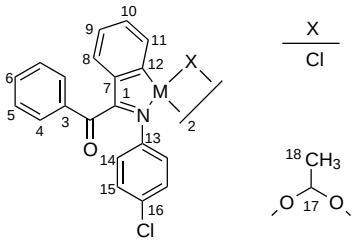

carbon	**1**	**2**[b] (M = Pd)	**3**[c] (M = Pd)	**4**[c] (M = Pt)	**5**[b] (M = Pt)
C1	166.8	180.4	180.7	186.4 (89.5)	182.3 (41.6)
C2	197.0	191.8	191.9	191.5 (48.5)	192.0 (77.7)
C3	134.3	133.2	n.o.	133.0	131.9
C4,4′	128.0	129.2	129.4	129.5	129.1
C5,5′	128.7	129.2	129.6	129.4	129.1
C6	134.4	135.1	135.9	136.0	135.0
C7	134.6	145.5	145.5	144.3 (56.3)	144.9
C8	129.1	128.4	129.0	130.3 (36.1)	127.9
C9	128.8	124.5	124.8	124.7	126.2
C10	131.8	131.5	131.6	134.2 (41.6)	132.4
C11	128.8	133.2	136.0	133.8 (56.9)	133.2
C12	129.1	156.3	155.1	147.2 (1095.9)	140.7 (1183.2)
C13	147.6	143.0	143.4	143.1 (23.6)	143.1
C14,14′	121.7	125.7	126.1	126.7	123.1
C15,15′	128.0	127.8	128.1	127.7	129.1
C16	n.o.	132.8	133.0	131.7	n.o.
C17		n.o.			183.7
C18		23.8			23.5

[a] The numbers in parentheses correspond to $J(^{195}\text{Pt}-^{13}\text{C})$ in Hz; n.o. = not observed. [b] $CDCl_3$. [c] DMSO-d_6.

and platinum compounds are very similar, suggesting that they have analogous structures. The most significant differences between compounds **3** and **4** are observed in the C1 and C12 atoms directly involved in the cyclometalated ring. For the platinum derivatives, the largest shielding is observed in the C12 linked directly to the metal. These compounds exhibit a larger deshielding for C1. Both effects must be attributed to electronic perturbations due to the metal itself. On the other hand, the almost identical chemical shifts for C8, C9, and C10 in both types of compounds suggest that the palladium and platinum atoms have similar electronic back-bonding effects.

Crystal Structure of [Pd(4-ClC$_6$H$_4$N=C(COC$_6$H$_5$)C$_6$H$_4$)-(μ-OAc)]$_2$. The crystal structure of compound **2** is shown in Figure 1 together with the atomic numbering scheme. Significant bond distances and bond angles are listed in Table 3. The structure consists of discrete molecules separated by van der Waals distances without any element of symmetry. Each palladium atom is bonded in a distorted-square-planar coordination, approaching tetrahedral geometry, to the nitrogen atom, to the *ortho* carbon atom of the phenyl ring supporting the iminic carbon, and to one of the oxygen atoms from each of the two bridging acetates. The dihedral angles between planes N−Pd−C and O−Pd−O for Pd(1) and Pd(2) are 6.9 and 5.4°, respectively. The Pd−N and Pd−C bonds form the basis for a five-membered chelate ring. The bond lengths of Pd(1)−C(11) = 1.939(3) Å and Pd(2)−C(21) = 1.938(7) Å suggest the multiple-bond-like character of the Pd−C linkages due to metal-to-ligand back-bonding.[8] This conclusion is supported by the NMR data. The bond lengths of Pd(1)−N(1) = 2.017(2) Å and of Pd(2)−N(2) = 2.021(6) Å together with the Pd−C distances suggest an electronic delocalization in the five-membered ring. The Pd−O (Pd(1)−O(1) = 2.034(5) Å and Pd(2)−O(4) = 2.030(5) Å) bonds having nitrogen atoms in a *trans* position are significantly shorter than those showing a *trans* relationship with respect to the aromatic carbon (Pd(1)−O(3) = 2.123(5) Å and Pd(2)−O(2) = 2.131(5) Å), as a consequence of the different *trans* effects of both atoms.[15] All distances and angles within the acetate and the aromatic groups are normal. The Pd−Pd distance of 2.939(1) Å is within the range observed for other Pd complexes.[16] The iminic and carbonyl groups retain an almost orthogonal arrangement, as exhibited in the *N*-substituted α-benzoylbenzylideneamines.[17] The torsion angles N(1)−C(17)−C(18)−O(5) and N(2)−C(27)−C(28)−O(6) are 101.4 and −68.2°, respectively. The angle between the PdOONC planes is 36.4°. This angle is larger than that found in other

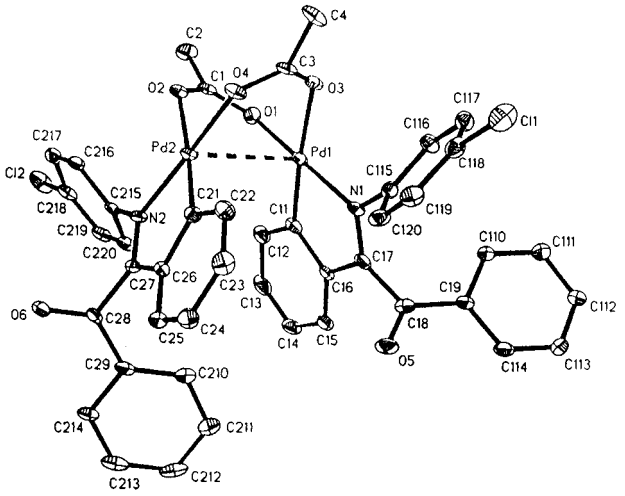

Figure 1. Diagram of the compound **2**. Thermal ellipsoids are at the 20% probability level.

Table 3. Selected Bond Distances and Angles for Compound **2**

	Distances (Å)		
Pd(1)−N(1)	2.017(2)	Pd(2)−N(2)	2.021(6)
Pd(1)−C(11)	1.939(3)	Pd(2)−C(21)	1.938(7)
Pd(1)−O(1)	2.034(5)	Pd(2)−O(4)	2.030(5)
Pd(1)−O(3)	2.123(5)	Pd(2)−O(2)	2.131(5)
N(1)−C(17)	1.311(9)	N(2)−C(27)	1.297(8)
C(17)−C(16)	1.44(1)	C(27)−C(26)	1.464(9)
C(17)−C(18)	1.49(1)	C(27)−C(28)	1.52(1)
C(16)−C(15)	1.39(1)	C(26)−C(25)	1.39(1)
C(15)−C(14)	1.38(1)	C(25)−C(24)	1.37(1)
C(14)−C(13)	1.36(1)	C(24)−C(23)	1.39(1)
C(13)−C(12)	1.41(1)	C(23)−C(22)	1.38(1)
C(12)−C(11)	1.40(1)	C(22)−C(21)	1.41(1)
C(16)−C(11)	1.43(1)	C(26)−C(21)	1.40(1)
O(1)−C(1)	1.271(9)	O(4)−C(3)	1.27(1)
C(1)−O(2)	1.233(9)	C(3)−O(3)	1.242(8)
C(1)−C(112)	1.51(1)	C(3)−C(212)	1.52(1)
C(18)−O(5)	1.21(1)	C(28)−O(6)	1.202(9)
C(18)−C(19)	1.47(1)	C(28)−C(29)	1.476(9)
Pd(1)−Pd(2)	2.939(1)		
	Angles (deg)		
O(1)−Pt(1)−O(3)	87.4(7)	O(4)−Pt(2)−O(2)	89.7(8)
O(1)−Pd(1)−O(3)	91.6(2)	O(4)−Pd(2)−O(2)	89.7(2)
C(11)−Pd(1)−O(1)	92.3(3)	C(21)−Pd(2)−O(4)	91.7(3)
N(1)−Pd(1)−O(3)	94.5(2)	N(2)−Pd(2)−O(2)	97.3(2)
N(1)−Pd(1)−C(11)	81.4(3)	N(2)−Pd(2)−C(21)	81.1(3)
Pd(1)−N(1)−C(17)	115.6(5)	Pd(2)−N(2)−C(27)	114.8(4)
N(1)−C(17)−C(16)	114.6(6)	N(2)−C(27)−C(26)	116.0(6)
C(17)−C(16)−C(11)	114.4(6)	C(27)−C(26)−C(21)	112.5(6)
Pd(1)−C(11)−C(16)	113.7(5)	Pd(2)−C(21)−C(26)	117.1(6)

(13) Bax, A.; Morris, G. A. *J. Magn. Reson.* **1981**, *42*, 501.
(14) Sánchez-Farrando, F. *Magn. Reson. Chem.* **1985**, *23*, 185.
(15) Caygill, G. B.; Steel, P. J. *J. Organomet. Chem.* **1987**, *327*, 115.
(16) Vicente, J.; Chicote, M. T.; Martín, J.; Artiago, M.; Solans, X.; Font-Altaba, M.; Aguiló, M. *J. Chem. Soc., Dalton Trans.* **1988**, 141.
(17) Fonseca, I.; Martínez-Carrera, S.; García-Blanco, S. *Acta Crystallogr.* **1979**, *B35*, 2643; **1982**, *B38*, 2735.

Table 4. IC_{50} Values[a] of the Cyclometalated Compounds **2**−**5** and *cis*-DDP against MDA-MB 468 and HL-60 Human Cancer Cells

compd	MDA-MB 468	HL-60
cis-DDP	2.67 ± 0.13	2.07 ± 0.21
2	6.75 ± 0.57	6.35 ± 0.70
3	8.95 ± 0.42	8.37 ± 0.63
4	1.58 ± 0.09	1.37 ± 0.08
5	1.05 ± 0.08	0.82 ± 0.02

[a] Values are given as (mean) ± (standard deviation).

cyclometalated compounds with acetate bridges (24.46 and 23.96°, where the ligands are benzothiazole and benzoxazole, respectively).[18]

Antiproliferative Analysis. Table 4 shows the IC_{50} values (μM) of the cyclometalated compounds **2**−**5** and *cis*-DDP against MDA-MB 468 and HL-60 human cancer cells. The data show that there are not significative differences in the antiproliferative activity of all compounds against either the HL-60 or the MDA-MB 468 cell lines. It was observed, however, that the antiproliferative activity against both types of tumor cells of compounds **4** and **5**, which contain Pt in their molecular structures, is higher than that of compounds **2** and **3**, which contain Pd. In fact, compounds **2** and **3** exhibit IC_{50} values higher than those of *cis*-DDP. In contrast, the IC_{50} values obtained for compound **5** (1.05 and 0.82 μM for MDA-MB 468 and HL-60, respectively) and for compound **4** (1.58 and 1.37 μM for MDA-MB 468 and HL-60, respectively) are lower than those showed by *cis*-DDP[19] (2.67 and 2.07 μM for MDA-MB 468 and HL-60, respectively). We think that the large antiproliferative activity shown by the platinated compounds, particularly of compound **5**, may be due to the fact that this drug provokes extensive DNA conformational changes (see below). These changes may lead to blockage of several biological processes such as DNA replication and transcription, as has been proposed.[20]

DNA Metalation. In order to determine the amount of metal bound to DNA, a total refraction X-ray fluorescence analysis was performed. We observed that a DNA metalation plateau was reached at 24 h of incubation with compounds **2**−**5** and *cis*-DDP at $r_i = 0.10$ (r_i = metal/nucleotide molar ratio). It was observed, moreover, that at 24 h of incubation the r_b value (metal covalently bound to DNA) of complex **5**−DNA was 1 order of magnitude superior to that of complex **4**−DNA ((76.58 ± 0.28) × 10^{-3} and (6.58 ± 0.24) × 10^{-3}, respectively), while the r_b value of *cis*-DDP−DNA complex is close to 0.1 ((99.60 ± 7.80) × 10^{-3}). The differences in r_b between both complexes may be a consequence of the differences in lability of the salient groups (chloride or acetate). It is likely that the high antiproliferative activity of compounds **4** and **5** may not be exclusively dependent on DNA metalation, since DNA metalation due to compound **4** is significantly lower than that due to compound **5**. The total X-ray fluorescence data indicated, on the other hand, that the Pd compounds **2** and **3** do not interact with the DNA through covalent interactions, because no Pd was detected in any case. These data were confirmed by CD spectroscopy, which showed that the CD spectra of EtOH-precipitated Pd complexes were identical with the CD spectra of the native DNA. In contrast, the CD spectra of EtOH-precipitated Pt complexes were identical with those of the native complexes (data not shown) as an indication of covalent binding of the metal to DNA.

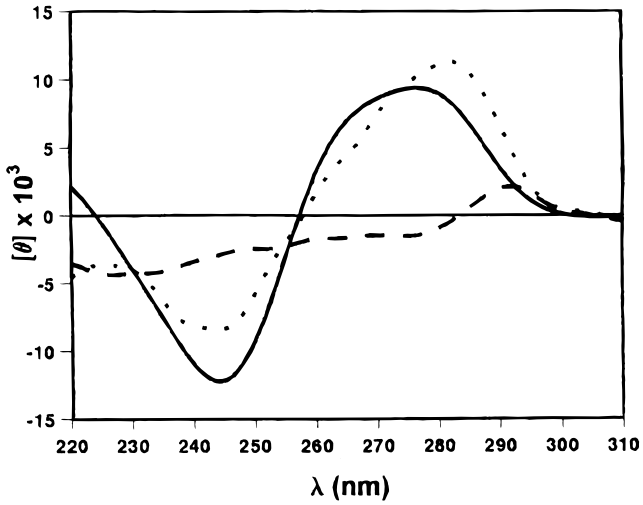

Figure 2. CD spectra of CT DNA incubated with compound **5**: (—) CT DNA; (•••) $r_i = 0.01$; (- - -) $r_i = 0.10$.

Table 5. CD Spectral Data for CT DNA Incubated with Compound **5**

compd	r_i	θ_{max}	λ_{max}	θ_{min}	λ_{min}
CT DNA[b]		9.38	276	−12.20	244
5−DNA	0.01	11.31	282	−8.39	244
5−DNA	0.10	2.12	292		

[a] θ in units of 10^3 deg cm^2 dmol^{-1}; λ in units of nm. [b] DNA control.

Table 6. UV Data and ΔT_m Values of CT DNA Incubated with Compound **5**[a]

compd	r_i	λ_{max}	$OD_{260\ nm}$	H (%)	ΔT_m
CT DNA[b]		258	0.500		
5−DNA	0.01	257	0.516	3.2	−5.5
5−DNA	0.10	257	0.596	19.2	−4.0

[a] λ in units of nm; ΔT_m in units of °C. [b] DNA control.

Circular Dichroism of the 5−DNA Complex. Since compound **5** shows high antiproliferative activity and it binds covalently to DNA, we have performed experiments to analyze the type of modifications induced upon binding of this compound to DNA. The CD spectra and the wavelengths at which the maximum and minimum values of ellipticity appear in control CT DNA and in CT DNA incubated at $r_i = 0.01$ and 0.10 are shown in Figure 2 and Table 5. It was observed that the maximum difference in the ellipticity value of the positive band relative to control CT DNA was obtained at $r_i = 0.10$ since from a value of 9.38 units in control CT DNA at 276 nm, a value of 2.12 units was observed in compound **5**−DNA at 292 nm. Moreover, the negative band was not observed, as a further indication of the large distortion of the helix at this r_i value. At lower r_i this distortion did not occur. There is an isodichroic point at 255 nm, although at $r_i = 0.10$ the distortion of the helix is quite drastic. The modification in the CD spectrum induced by compound **5** suggests that a certain opening and rotation of the bases in the DNA by this compound must occur, since the CD spectral changes observed indicate relaxation of the original B-DNA form.

UV Behavior of the 5−DNA Complex. Table 6 shows that cyclometalated compound **5** induces alteration of the DNA secondary structure, since a hyperchromic effect at 260 nm and variations in the value of λ_{max} were detected. Compound **5** induces a higher hyperchromic effect at $r_i = 0.10$. Table 6 also shows the T_m increase induced by compound **5** after 24 h of complex formation at $r_i = 0.01$ and 0.10. It can be observed that the compound induces a destabilizing effect on DNA higher

(18) Churchill, M. R.; Wassermann, M. J.; Young, G. J. *Inorg. Chem.* **1980**, *19*, 762.
(19) Farrell, N. *J. Med. Chem.* **1989**, *32*, 2240.
(20) Umapathy, P. *Coord. Chem. Rev.* **1989**, *95*, 129.

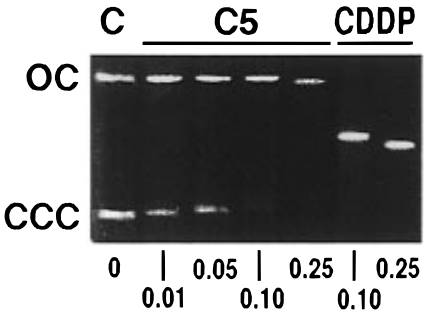

Figure 3. Changes in the electrophoretic mobility of the ccc (covalently closed circular) and oc (open circular) forms of native pUC8 plasmid DNA after incubation with compound **5**: (lane 1) control; (lanes 2−5) compound **5**; (lanes 6 and 7) *cis*-DDP.

than that induced by *cis*-DDP.[21] In fact, while the T_m value of native DNA is 62 °C, the T_m value of compound **5**−DNA formed at $r_i = 0.01$ decreases to 56.5 °C ($\Delta T_m = -5.5$ °C). The T_m value increases to 58 °C ($\Delta T_m = -4$ °C) at $r_i = 0.10$. It is interesting to note that when r_i increases from 0.01 to 0.10 in complex **5**−DNA, a T_m increment of 1.5 °C is observed, in contrast with what was detected for *cis*-DDP. The decrease in T_m of the DNA due to compound **5** binding probably results from intrastrand adduct formation in a similar way as for *cis*-DDP, since it has been shown that these kinds of adducts are responsible for DNA destabilization.[22]

Electrophoretic Behavior of Drug−DNA Complexes. The analysis of the influence of compound **5** on the tertiary structure of DNA was determined by its ability to alter the electrophoretic mobility of the covalently closed circular (ccc) and open circular (oc) forms of pUC8 plasmid DNA. Figure 3 shows the mobility of native pUC8 plasmid DNA and of plasmid DNA incubated with compound **5** at $r_i = 0.01$, 0.05, 0.10, and 0.25, and with *cis*-DDP at $r_i = 0.10$ and 0.25. It was observed that as the r_i value increases, incubation of the DNA with compound **5** gradually induces a decrease in mobility of the ccc form and an increase in mobility of the oc forms of pUC8 DNA. It is likely that the decrease in mobility of the supercoiled DNA must be attributed to unwinding of the superhelix. The increase in mobility of the oc form might possibly be associated with a DNA-shortening effect.[23,24] The changes in mobility due to *cis*-DDP binding are slightly higher than those due to compound **5**. The lower level of DNA uncoiling relative to *cis*-DDP shown by compound **5** may be explained either by less bending of the double helix (less than 42°) due to intrastrand bifunctional adducts or by a lower level of DNA binding and intrastrand monofunctional DNA adducts imposed by the bulky cyclometalated residues in compound **5**.

Interstrand Cross-Link Formation. Since gel electrophoresis experiments suggested that compound **5** induces DNA intrastrand drug−DNA adducts in a way similar to that of *cis*-DDP, we further tested whether compound **5** is also able to induce interstrand cross-links. Figure 4 shows the pattern of DNA bands of linear pF18 plasmid DNA incubated with compounds **5** and *cis*-DDP at $r_i = 0.10$ for different periods of time. Figure 4 shows that native linear pF18 melted DNA migrates as a band which corresponds to the single-stranded DNA form (lane 2). As expected, upon *cis*-DDP binding there is a gradual increase in the double stranded form. After 6 h of incubation with the drug, most of the DNA migrates as the double-stranded form (lane 6) as an indication of interstrand cross-link formation. A quantitative analysis of the autorradiographs indicated that after 3 and 6 h of incubation of the DNA with *cis*-DDP about 20% and 100% of the DNA remained in the double-stranded form. In contrast, compound **5** did not induce interstrand cross-linking, since all the DNA remained in the single-stranded form.

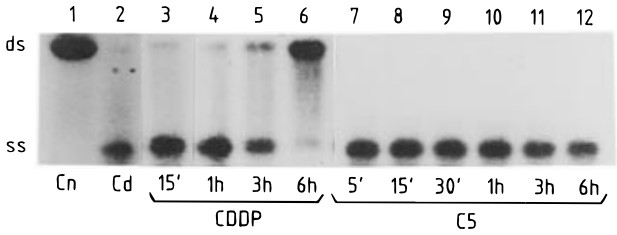

Figure 4. Pattern of DNA bands of linear pF18 plasmid DNA incubated with compound **5** and *cis*-DDP at $r_i = 0.10$ for different periods of time. (lanes 1 and 2) control; (lanes 3−6) *cis*-DDP; (lanes 7−12) compound **5**. Legend: ds = double strand, ss = single strand; Cn = native DNA, Cd = denatured DNA.

Conclusion. In view of these results we think that the biochemical activity of compound **5** must be attributed to covalent binding to DNA, forming mono- or bifunctional Pt−DNA adducts, which in turn induces important modifications of the helix. We suggest that compound **5** induces intrastrand adducts in way similar to that for *cis*-DDP.

III. Experimental Section

General Procedures. The infrared spectra were recordered in Nujol mulls and KBr pellets in the 4000−200 cm^{-1} range using a Perkin-Elmer Model 283 spectrophotometer. NMR spectra were recordered on a Bruker WP-200-SY (200 MHz) spectrometer in $CDCl_3$ with TMS as internal standard and in DMSO-d_6. The C, H, and N analyses were carried out in a Perkin-Elmer 240B microanalyzer. All solvents were purified, prior to use, by standard methods.[25] $Pd(OAc)_2$ and K_2PtCl_4 were purchased from Strem and Johnson Matthey, respectively. Ligand **1** (L; *N*-(4-chlorophenyl)-α-benzoylbenzylideneamine) was synthesized as previously described.[26]

Synthesis of [PdL(μ-OAc)]$_2$ (2). A mixture of equimolar amounts of $Pd(OAc)_2$ and L in HOAc was heated at 50 °C under nitrogen for 2 h. After removal of the solvent in vacuo the residue was extracted with CH_2Cl_2. The elution with CH_2Cl_2−EtOH (1%) gave the desired complex **2** (yield 56%). Anal. Calcd for $C_{44}H_{32}N_2O_6Cl_2Pd_2$: C, 54.56; H, 3.31; N, 2.89. Found: C, 54.51; H, 3.32; N, 2.92. IR (ν_{max}, cm^{-1}): C═O, 1672; C═N, 1598; C−O_{acet} 1584, 1418; Pd−N, 450; Pd−C, 610. ^1H NMR ($CDCl_3$, δ (ppm)): 7.72−6.80 (m, 9H, aromatic protons), 6.93 and 6.65 (AA′BB′, 4H), 1.80 (s, 3H, OAc).

Synthesis of [PdL(μ-Cl)]$_2$ (3). Method A. To a solution of the acetate-bridged dimer (compound **2**) in acetone was added an equimolar amount of NaCl. The solid obtained (compound **3**) was filtered and dried in vacuo (yield 78%).

Method B. A mixture of equimolar amounts of $PdCl_2$ and of L in MeOH was stirred for 2 days at 25 °C. The solid obtained (compound **3**) was filtered and dried in vacuo (yield 40%). Anal. Calcd for $C_{40}H_{26}N_2O_2Cl_4Pd_2$: C, 52.14; H, 2.82; N, 3.04. Found: C, 52.09; H, 2.79; N, 3.03. IR (ν_{max}, cm^{-1}): C═O, 1673; C═N, 1594; Pd−N, 451; Pd−C, 606; Pd−Cl, 319, 295.

Synthesis of [PtL(μ-Cl)]$_2$ (4). To a solution of bis(μ-chloro)bis-[(η^3-2-methylallyl)platinum] in $CHCl_3$ was added 2 equiv of L. This mixture was refluxed until a precipitate was formed. The precipitate was filtered, washed with $CHCl_3$ and ether, and dried in vacuo (yield 62%). Anal. Calcd for $C_{40}H_{26}N_2O_2Cl_4Pt_2$: C, 43.72; H, 2.37; N, 2.55.

(21) Eastman, A. *Biochemistry* **1983**, *22*, 3927.
(22) Johnson, N. P.; Lapetoule, P.; Razaka, H.; Villani, G. In *Biochemical Mechanisms of Platinum Antitumor Drugs*; McBrien, D. H. C., Slater, T. F., Eds.; IRL Press: Oxford, U.K., 1986; pp 1−28.
(23) Cohen, G. L.; Lippard, S. J. *Science* **1979**, *203*, 1014.
(24) Hermans, T. S.; Teicher, B. A.; Chan, V.; Collins, L. S. *Cancer Res.* **1988**, *48*, 2335.
(25) Perrin, D. D.; Armarego, W. L. F.; Perrin, D. R. *Purification of Laboratory Chemicals*, 2nd ed.; Pergamon Press: Oxford, U.K., 1980.
(26) Alcaide, B.; León-Santiago, M. A.; Pérez-Ossorio, R.; Plumet, J.; Sierra, M. A.; De la Torre, M. *Synthesis* **1982**, 989.

Table 7. Crystal Analysis Parameters of Compound **2**

Crystal Data	
formula	$C_{44}H_{32}N_2O_6Cl_2Pd_2 \cdot C_4H_{10}O$
sym	triclinic, *P*1
unit cell determination	least-squares fit from 25 rflns
unit cell dimens	
a	11.765(3) Å
b	12.862(4) Å
c	15.022(5) Å
α	84.08(2)°
β	78.56(2)°
γ	83.13(2)°
packing	
V, *Z*	2204(11) $Å^{-3}$, 2
D_c, *F*(000)	1.570 g cm^{-3}, 1052
μ	0.991 mm^{-1}
Experimental Data	
diffractometer used	Stoe four-circle
radiation	Mo Kα ($\lambda = 0.710\ 73$ Å)
temp	180 K
monochromator	highly oriented graphite cryst
scan type	*ω*/*θ*
no. of rflns	
measd	6164
obsd	4720 ($F > 4.0\sigma(F)$)
range of *hkl*	−12 to +12, −13 to +13, −10 to +16
std rflns	3 measd every 100 rflns, no variation
Solution and Refinement	
system used	Siemens SHELXTL PLUS (PC version)[a]
soln	direct methods
refinement	full-matrix least squares
H atoms	riding model, fixed isotropic *U*
weighting scheme	$w^{-1} = \sigma^2(F) + 0.0050F^2$
final ΔF_o peaks (e $Å^{-3}$)	1.37
final *R* and R_w	0.063, 0.084
scattering factors	*b*
anomalous dispersion	*b*

[a] SHELXTL PLUS, program version 4.0, Siemens Analytical Instruments, Madison, WI, 1990. [b] *International Tables of X-ray Crystallography*; Kynoch Press: Birmingham, U.K., 1974; Vol. IV, pp 99−100, 149.

Found: C, 43.68; H, 2.33; N, 2.52. IR (ν_{max}, cm^{-1}): C═O, 1672; C═N, 1595; Pd−N, 453; Pd−C, 616; Pt−Cl, 328, 324.

Synthesis of [PtL(*μ*-OAc)]$_2$ (5). To a suspension of [PtL(*μ*-Cl)]$_2$ in $CHCl_3$ was added an equimolar amount of AgOAc. The whitish solution changed to red in 10 min. Afterward, the solution was filtered and concentrated. A deep red solid product precipitated after addition of MeOH (yield 78%). Anal. Calcd for $C_{44}H_{32}N_2O_6Cl_2Pt_2$: C, 46.11; H, 2.79; N, 2.44. Found: C, 46.07; H, 2.80; N, 2.42. IR (ν_{max}, cm^{-1}): C═O, 1672; C═N, 1595; C−O_{acet}, 1584, 1424; Pd−N, 452; Pd−C, 615 cm^{-1}. ^{1}H NMR ($CDCl_3$, *δ* (ppm)): 7.64−6.60 (m, 13H, aromatic protons), 1.95 (s, 3H, OAc).

Structural Determination and Refinement of Compound 2. Orange crystals were obtained after recrystallization of compound **2** by slow evaporation from a CH_2Cl_2−EtOH (1%) solution. Intensity data were recorded on a Stoe four-circle diffractometer using graphite-monochromated Mo Kα ($\lambda = 0.710\ 73$ Å) radiation. The data, the details of the data collection, and the structural analysis are summarized in Table 7. Three standard reflections were measured every 100 reflections. There was no evidence of crystal decomposition. The data were corrected for absorption. They were averaged to give 4720 unique observed reflections with $F > 4\sigma(F)$. The structure was solved by direct methods, and refinement, based on F^2, was by full-matrix least-squares techniques.[27] All non-H atoms were refined anisotropically until $R = 0.063$. H atoms were placed in idealized positions and allowed to ride on the relevant C atom; C−H = 0.96 Å. A Et_2O solvate molecule was located.

(27) (a) Sheldrick, G. M. SHELXS86: Program for the Solution of Crystal Structures; University of Göttingen, Göttingen, Germany, 1985. (b) Sheldrick, G. M. SHELXL93: Program for the Refinement of Crystal Structures; University of Göttingen, Göttingen, Germany, 1993.

Biological Assays. Formation of Drug−DNA Complexes. Stock solutions of each compound (1 mg/mL) were stored in the dark at room temperature until use. Drug−DNA complex formation was accomplished by addition to CT DNA (calf thymus DNA, purchased from Sigma) of aliquots of each of the compounds at different concentrations in 0.02 SSPE (SSPE = 180 mM NaCl, 10 mM NaH_2PO_4, 1 mM EDTA, pH 7.0). The amount of drug added to the DNA solution was expressed as r_i (the input molar ratio of Pt or Pd to nucleotides). The mixture was incubated at 37 °C for various periods of time, as indicated below.

Cytotoxicity Assays. MDA-MB 468 cells were grown in DMEM medium without sodium pyruvate and with glucose (4.5 g/L), supplemented with 10% FCS (fetal calf serum), 10 *μ*g/mL of insulin, and 1% antibiotic−antimycotic solution. The replication period of MDA-MB 468 cells was 24 h at 37 °C under an atmosphere with 5% CO_2, reaching the logarithmic growth phase at 72 h. HL-60 cells were cultured in RPMI 1640 medium suplemented with 10% FCS and 1% antibiotic−antimycotic solution. The replication period of HL-60 cells was 16 h, reaching the logarithmic growth phase at 48 h under an atmosphere of 5% CO_2. In order to calculate the concentration of the compounds which produces 50% inhibition of cell growth (IC_{50}), 200 *μ*L aliquots of cell culture (2.5×10^5 cells/mL) were incubated with the compound at concentrations between 0 and 100 *μ*g/mL for 48 h (HL60 cell line) or 72 h (MDA-MB 468 cell line). Cell density was determined in control and drug-treated cultures using a Neubauer haemocitometer. Data were obtained from survival curves in which the percentage of cell survival was plotted against the logarithm of drug concentration. All experiments were carried out in triplicate.

Quantitation of Pt/Pd Binding to DNA. A 20 *μ*g/mL solution of CT DNA in TE buffer (10 mM Tris·HCl, pH 8.0, 0.1 mM EDTA) was incubated at 37 °C with the drugs at $r_i = 0.10$. After 24 h of incubation, the DNA was precipitated twice with 2.5 volumes of cold ethanol and 0.1 volume of 3 M NaAc, pH 4.8. The DNA was washed with 70% ethanol and resuspended in 1 mL of TE buffer. The amount of DNA in each sample was measured by UV spectrophotometry (Beckman Acta cIII) at 260 nm. The percentage of metal covalently bound to DNA was determined by total X-ray fluorescence (TXRF) using a Seifert EXTRA-II apparatus. As controls, Pt and Pd determinations were also made in native DNA and in DNA precipitated immediately after addition of the compounds. The assays were made in triplicate.

Circular Dichroism Spectroscopy. The CD spectra were performed in a 1 cm rectangular quartz cell in a JASCO J-600 spectropolarimeter attached to a temperature programmer using a computer for spectral subtraction and noise reduction. The CD analysis was done at 20 °C. Each sample was scanned twice in a range of wavelengths between 220 and 310 nm. The generated CD spectra represent the mean of three independent scans.

Ultraviolet Spectral Data. UV measurements of the drug−DNA complexes (20 *μ*g/mL of DNA, $r_i = 0.01$ and 0.10) were carried out at 25 °C by differential spectrophotometry in a Shimadzu PR-1 spectrophotometer. The T_m values of native DNA and compound **4**−DNA and compound **5**−DNA complexes (20 *μ*g/mL) were recorded at 260 nm by differential spectrophotometry at an increase rate of 1 °C/min from 45 to 95 °C in a Beckman Acta cIII spectrophotometer attached to a temperature programmer. The maximum value of hyperchromicity in control DNA at 95 °C was 33%. The data represent the mean values of three independent determinations.

Gel Electrophoresis of Drug−pUC8 Complexes. pUC8 DNA aliquots (50 *μ*g/mL) were incubated with the drugs in a buffer solution containing 50 mM NaCl, 10 mM Tris·HCl (pH 7.4), and 0.1 mM EDTA at several r_i values. Incubations were performed in the dark at 37 °C. Aliquots (20 *μ*L) of the drug−DNA complexes containing 1 *μ*g of DNA were subjected to 1.5% agarose gel electrophoresis for 16 h at 25 V in 40 mM Tris·acetate and 2 mM EDTA pH 8.0 buffer. The DNA was stained with ethidium bromide (0.5 *μ*g/mL). The gels were photographed with a MP-4 Polaroid camera using 665 Polaroid film and an orange filter.

Interstrand Cross-Link Assay. The pF18 plasmid DNA was linearized by digestion in 150 mM NaCl with 10 units/*μ*g of DNA of Bam HI at 37 °C for 4 h. pF18 DNA was 3′-end labeled by incubation with 2.5 *μ*Ci/*μ*g of DNA of [α-^{32}P]dCTP and 1.25 units/*μ*g of DNA of Klenow fragment of *Escherichia coli* DNA pol I for 30 min at room temperature. The reaction was stopped by heating to 70 °C for 5 min.

Unincorporated radioactivity and proteins were removed by passing the labeling reaction mixture through a Sephadex G-50 column. Sonicated CT DNA was added to the eluted solution of labeled pF18 DNA to a final DNA concentration of 180 μg/mL. DNA at a concentration of 90 μg/μL was incubated with the drug in Bam HI buffer (150 mM NaCl) at $r_i = 0.10$. Aliquots (10 μL) were removed after several periods of incubation (5 min, 15 min, 30 min, 1 h, 3 h, and 6 h for compound **5** and 15 min, 1 h, 3 h, and 6 h for *cis*-DDP), and the reaction was terminated by addition of an equal volume of loading dye (90% formamide, 10 mM EDTA, 0.1% xylene cyanol, and 0.1 bromophenol blue). DNA was melted for 10 min at 90 °C, and samples were chilled on ice prior to loading onto 1% agarose gel. Electrophoresis was carried out in agarose gel in TAE buffer at 20 V for 16 h. The gel was dried and autoradiographed. The density of the bands was determined in a Molecular Dynamics Computing Densitometer (Model 300A).

Acknowledgment. We thank the CICYT (Grant Nos. SAF 93-1122, HB-059, SAF 93-0140, and CAM 160/92) for financial support. We thank Johnson-Matthey Ltd. for their generous loan of K_2PtCl_4.

Supporting Information Available: Listings of atomic coordinates, anisotropic thermal parameters for non-hydrogen atoms, positional and isotropic thermal parameters for hydrogen atoms, and all bond distances and angles for **2** (8 pages). Ordering information is given on any current masthead page.

IC960050Y